REPORT DOCUMENTATION PAGE

1. REPORT DATE *(DD-MM-YYYY)*	2. REPORT TYPE	3. DATES COVERED *(From - To)*
10/13/2005	Final Report	07/22/02-07/21/05

4. TITLE AND SUBTITLE	5a. CONTRACT NUMBER
Promotion or Retention of Desired Metastable and Ultrafine Microstructures with an Electric Field or Current	DAAD19-02-1-0315
	5b. GRANT NUMBER
	5c. PROGRAM ELEMENT NUMBER

6. AUTHOR(S)	5d. PROJECT NUMBER
H. Conrad, K. Jung and J. Narayan	
	5e. TASK NUMBER
	5f. WORK UNIT NUMBER

7. PERFORMING ORGANIZATION NAME(S) AND ADDRESS(ES)	8. PERFORMING ORGANIZATION REPORT NUMBER
North Carolina State University Materials Science and Engineering Campus Box 7919 Raleigh, NC 27695-7919	5-21616F

9. SPONSORING/MONITORING AGENCY NAME(S) AND ADDRESS(ES)	10. SPONSOR/MONITOR'S ACRONYM(S)
U. S. Army Research Office P. O. Box 12211 Research Triangle Park, NC 27709-2211	ARO
	11. SPONSORING/MONITORING AGENCY REPORT NUMBER 41893.29-MS

12. DISTRIBUTION AVAILABILITY STATEMENT
Approved for public release; distribution unlimited.

13. SUPPLEMENTARY NOTES
The views, opinions and /or findings contained in this report are those of the author(s) and should not be construed as an official Department of the Army position, policy or decision, unless so designated by other documentation.

14. ABSTRACT
The influence of an electric field on the equlibria and kinetics of grain growth and phase transformations in metals and the resulting mechanical properties were determined, with attention to ultrafine and nanometer microstructures. The phenomena and materials considered were: (a) precipitation in Al-Mg-Si alloys, (b) phase coarsening in 60Sn40Pb solder joints, (c) grain growth in electrodeposited Cu and (d) dependence of the plastic flow stress on grain size. Regarding (a), a field applied during solutionizing increased the solubility of the pertinent constituents and in turn the tensile properties in the naturally-aged temper. Thermodynamic considerations along with HRTEM and SAED studies indicated that the field reduced the Gibbs free energy of solution, increased the size of the naturally-aged precipitates and changed their crystal structure. Regarding (b), a field retarded coarsening of the Sn and Pb phases and changed

15. SUBJECT TERMS
Electric field, solubility, phase transformations, grain growth, precipitates, phase coarsening, pulsed laser vapor deposition, heterojunctions, nanodot structure.

16. SECURITY CLASSIFICATION OF:			17. LIMITATION OF ABSTRACT	18. NUMBER OF PAGES	19a. NAME OF RESPONSIBLE PERSON
			UL	25	Prof. Hans Conrad
a. REPORT unclassified	**b. ABSTRACT** unclassified	**c. THIS PAGE** unclassified			**19b. TELEPONE NUMBER** *(Include area code)* 919.515.7443

14. ABSTRACT (Continued)

their volume fractions. The effect of the field on phase coarsening appeared to be through its effect on the diffusion coefficient. Regarding (c), a field retarded grain growth. Whether the field retarded grain boundary mobility or enhanced the annihilation of the crystal defects responsible for the driving force was not clear. Regarding (d), analysis of the effect of grain size d on the flow stress of metals and compounds over the range from nanometers to millimeters indicated three regimes: Regime I ($d > \sim 10^{-6}$m), Regime II ($d \approx 10^{-8}$-10^{-6}m) and Regime III ($d < 10^{-6}$m). Dislocations are active in I and II and obscent in III. The mechanism governing Regime III appears to be grain boundary shear accommodated by grain boundary diffusion.

Unique pulsed laser vapor deposition techniques were employed to fabricate: (a) metals and compounds with nanometer grain size, (b) $La_{0.7}Sr_{0.3}MnO_3$/ZnO heterostructures and (c) nanodot metals embedded in ceramic matrices, and their respective novel mechanical or electrical properties were determined.

Final Report

PROMOTION OR RETENTION OF DESIRED METASTABLE AND ULTRAFINE MICROSTRUCTURES WITH AN ELECTRIC FIELD OR CURRENT

ARO Contract/Grant Number: DAA19-02-1-0315

Table of Contents

List of Appendixes

1. Statement of Problem Studied

Materials science deals with the production and control of microstructure having the aim of optimizing or improving the properties of materials. Of considerable interest in recent years has been the development of metals and ceramics with an ultrafine microstructure extending into the nanometer range. In view of the high internal energy associated with the interfaces in such ultrafine microstructures, they tend to be unstable and coarsen, thereby losing beneficial properties. *Desirable therefore are means for promoting and retaining desired metastable and ultrafine microstructures*

The external parameters generally employed in the processing and control of microstructures in materials are: (a) temperature, (b) pressure or stress, (c) environment (gas, liquid or solid) and (d) time. Usually neglected are electric and magnetic fields. However, it has been shown in previous work by the PI (H. Conrad) sponsored by ARO that electric fields can have a significant influence on the properties of metals, even though an effect is not expected. *The major objective of the present study was therefore to further evaluate the effects of an electric field on the microstructure of metals, with the aim of promoting or retaining desired metastable and ultrafine microstructures.*

2. Summary of the Most Important Results

2.1 Precipitation Hardening of Al Alloys: The alloys investigated were the commercial age-hardening Al-Mg-Si alloys AA6061, 6022 and 6111 with the compositions given in Table 1. They are based on the precipitate Mg_2Si and are finding increasing application in the automotive and aerospace industries. Alloy 6061 is a

1

Table 1. Pertinent alloying constituents in wt.% in three 6××× Al-Mg-Si alloys.

Alloy	Mg_2Si	Excess Si	Cu
6061	1.51	0.07	0.01
6022	0.92	0.40	0.06
6111	1.23	0.19	0.79

nominally balanced Mg_2Si alloy, 6022 has an excess of Si and 6111 has the addition of

Cu. The solubility of the pertinent solutes during the solution heat treatment (SHT) and

the subsequent natural aging behavior of these alloys were monitored by conductivity Σ

(resistivity $\rho = \Sigma^{-1}$) and Vickers hardness H_v measurements of water-quenched specimens.

Tensile properties (YS, TS and % El.) were determined at the peak naturally-aged

condition (T4 temper).

It was found that the application of an external dc electric field E during SHT at

450°-550°C of 6022 and 6111 decreased both the enthalpy ΔH_s and entropy ΔS_s of

solution with a resulting decrease in the Gibbs free energy $\Delta G_s = \Delta H_s - T\Delta S_s$, giving an

increase in the solubility of Mg_2Si; see Fig. 1. The equations by which the solubility of

Mg_2Si was determined from the resistivity ρ and hardness H_v measurements are given in

Appendix I. The influence of alloy composition on the increase in solubility produced by

the electric field is shown in Fig. 2. This shows that the increase depends on the presence

of excess Si and the addition of Cu in the Al-Mg-Si alloys, which accounts for the fact

that the field had no detectable effect on the 6061 alloy.

The dependence of the thermodynamic parameters of ΔH_s, ΔS_s and ΔG_s on the

strength of the electric field is shown in Fig. 3. All three parameters decrease with field
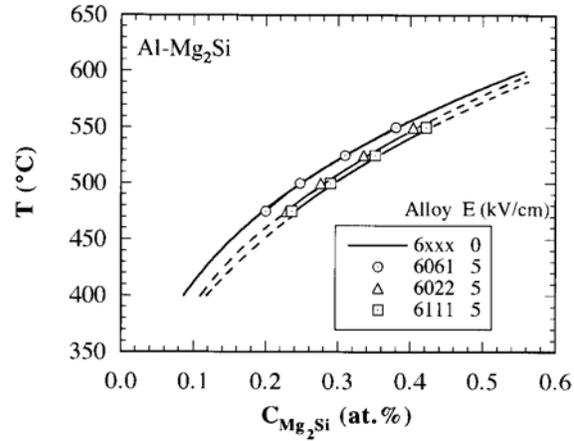
Fig. 1. Increase in the solubility of Mg₂Si in Al-Mg-Si alloys by application of an electric field during solution heat treatment. The solubility in 6××× alloys with E=0 taken from Gröng [1].
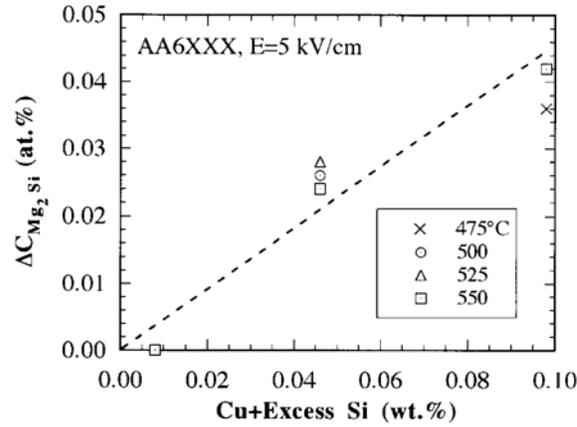
Fig. 2 . Effects of Cu + excess Si on the increase in solubility Δc of Mg₂Si at 475°-550°C produced by application of an electric field E=5 kV/cm.

strength up to ~1 kV/cm and then only slightly, if at all, at higher field strengths. The increase in solubility with field strength is given by (see Appendix I)

$$\overline{D}^{m} - \overline{D}_{o}^{m} = k_{o}\exp(-Q/RT)t \qquad (3)$$

where c_{Mg_2Si} is the concentration of Mg₂Si and $\Delta G_s(E)$ decreases with field strength E according to Fig. 3.

3
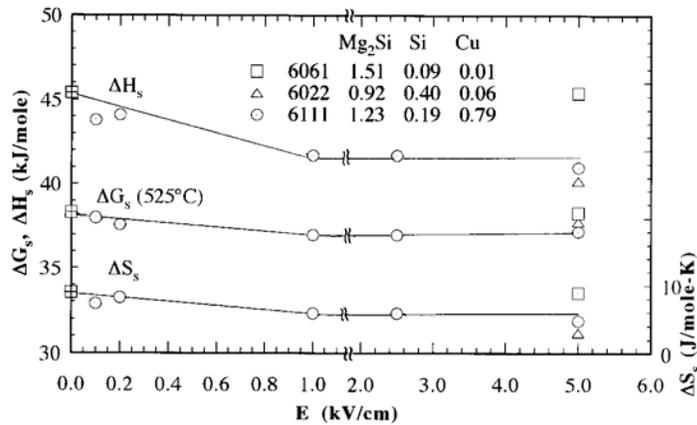
Fig. 3. The effect of the electric field strength on the enthalpy ΔH_s, entropy ΔS_s, and Gibbs free energy $\Delta G_s = (\Delta H_s - T\Delta S_s)$ of solution of Mg_2Si in three Al-Mg-Si alloys 6061, 6022 and 6111.

The increase in ρ (and in H_v) which resulted from the increase in solubility by the application of a field during SHT prevailed throughout the subsequent natural aging process; see for example Fig. 4. An analysis of the kinetics of the natural aging process in terms of the Johnson-Mehl-Avrami-Kolmogorov (JMAK) model [2-4] (Appendix II) gave that the application of the field during SHT had no clear effect on the subsequent natural aging kinetics.

The effect of applying an electric field during SHT at 475°-550°C on the tensile properties in the T4 temper (naturally-aged for 1mo.) of 6111 is shown in Fig. 5. An increase in tensile properties with application of a field is clearly evident. *Of special note is that the application of only 200 V/cm during SHT at 500°C gave tensile properties equivalent to those at 550°C without a field. Reductions of 10°-20°C in the normal SHT temperature were obtained for 6022. Decreases in the SHT temperature of these magnitudes offer the potential for considerable savings in industrial SHT practice.*
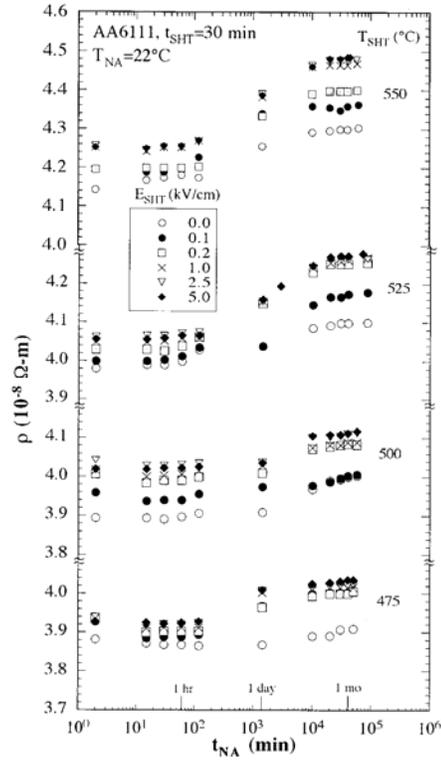
4

Fig. 4. Increase in resistivity ρ with natural aging time t_{NA} as a function of the field strength E_{SHT} applied during the solution heat treatment of 6111 at 475°-550°C.
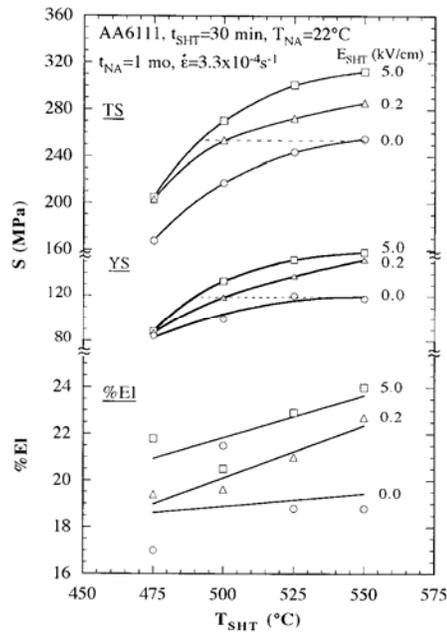

Fig. 5. Tensile properties of the 6111 alloy naturally-aged for 1 mo (T4 temper) as a function of the electric field strength applied during solution heat treatment at 475°-550°C.

Of interest is the change in microstructure which leads to the improved tensile properties in the T4 temper as a result of the application of an electric field during processing. For this, high resolution transmission electron microscopy (HRTEM) observations and selected area electron defraction (SAED) studies were performed on 6022 specimens which had been; (a) SHT at 525°C and naturally-aged for 2-3 yr without an electric field and (b) SHT with E=5 kV/cm plus an initial natural aging treatment (INA) for 15 min with E=5 kV/cm immediately following the water quench and (c) subsequently naturally-aged for 2-3 yr without a field. The application of the field during the initial natural aging (INA) as well as during SHT further enhanced slightly the tensile properties over those for applying the field only during SHT.

Examples of the precipitates are given in Fig. 6. In general, the precipitates in the specimen processed with the field were larger and spaced further apart than those without field. Their size distributions are shown in Fig. 7. An analysis of the diffraction rings in corresponding SAED patterns indicated that the crystal structure of precipitates without
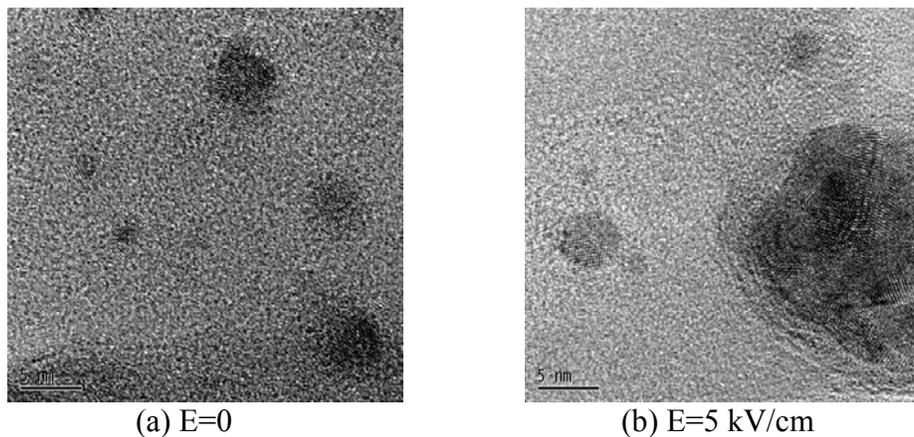

(a) E=0   (b) E=5 kV/cm

Fig. 6. HRTEM micrographs of 6022 solution heat treated for 10 min at 525°C, water quencher and naturally-aged for 2 yr: (a) E_{SHT}=0 and (b) E_{SHT}=5 kV/cm plus 15 min initial natural age (INA) with E_{INA}=5 kV/cm.
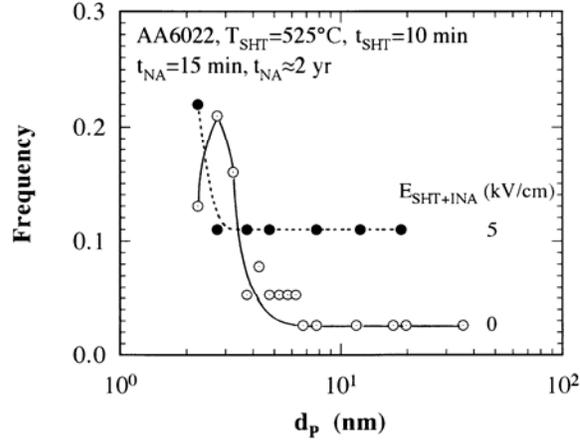
Fig. 7. Size distribution of the precipitates in 6022 naturally-aged for 2 yr which had been processed without and with E=5 kV/cm.

field was c-centered monoclinic β", while that with the field did not correspond

to any known crystal structure. *This is the first time that the size distribution and crystal*

structure of naturally-aged precipitates in an Al-Mg-Si alloy have been determined.

The increase in tensile properties with application of a field can be attributed to the

differences in the precipitate size, spacing, volume fraction and crystal structure. The yield

stress due to precipitates in the peak naturally-aged state (T4 temper) is given by [5]

$$\sigma_{ppt} = \frac{M(F^*)^{3/2} f_{ppt}^{1/2}}{b(2\sqrt{3}\pi)^{1/2} \Gamma^{1/2} r^*} \tag{2}$$

where M is the Taylor factor, F^* the interaction force between dislocations and the

precipitates with average size r^*, f_{ppt} the volume fraction of precipitates, b the Burgers

vector and Γ the dislocation line tension. According to Eqn. 2 an increase in yield stress

occurs when the product $[(F^*)^{3/2} f_{ppt}^{1/2}]/r^*$ increases. Considering the increase in yield

stress produced in the specimens processed with a field, it was found that although the

volume fraction of precipitates f_{ppt} increased with field, the corresponding increase in r^*

was such that the ratio $f_{ppt}^{1/2}/r^*$ decreased with field. Hence, *it appears that the field*

produced an increase in the interaction force F^* through its effect on the size and crystal

structure of the precipitates. This is turn gave the observed increase in yield stress.

2.2 Second Phase Coarsening: Solder joints in electronic packages frequently fail by low-

cycle fatigue. This fatigue mechanism is enhanced by the coarsening (which occurs during

operation) of the fine microstructure produced during the soldering operation. Of interest

was the influence of an electric field on the coarsening of the Sn and Pb phases in

60Sn40Pb solder joints with initial phase sizes of ~1 μm.

A reduction in the phase coarsening rate of both the Sn-rich phase and the Pb-rich

phase in 60Sn40Pb solder joints by the field is shown in Fig. 8. It was determined that the

reduction in coarsening rate corresponded to a decrease in the parameter m and the product

$k_o \exp(-Q/RT)$ in the usual coarsening equation

$$\overline{D}^m - \overline{D}_o^m = k_o \exp(-Q/RT)t \qquad (3)$$

where $\overline{D}$ is the average phase size, $\overline{D}_o$ the initial phase size, Q the activation energy, t the

time and k_o and m constants. The influence of the field on phase coarsening varied from

the outer surface to the center of the 4 mm dia solder joint, a greater retardation of the

coarsening occurring near the outer surface compared to the center; see Fig. 9. This

behavior is similar to that which occurred for the sintering of iron powder compacts [6],

where it was found that the reduction in porosity produced by a field was greatest near the

external surface. This was attributed to the migration of charged vacancies to the charged

8

surface produced by the field. *It was therefore concluded that the major effect of the field on phase coarsening in the 60Sn40Pb solder joints was through its reduction of the diffusion coefficient.*
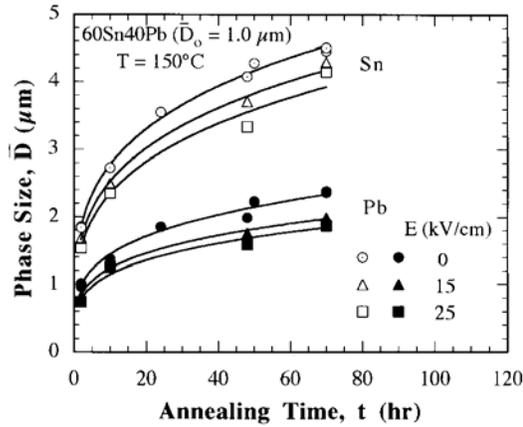
Fig. 8. Mean size D of the individual Pb and Sn phases in 60Sn40Pb solder joints vs annealing time at 150°C as a function of electric field strength.
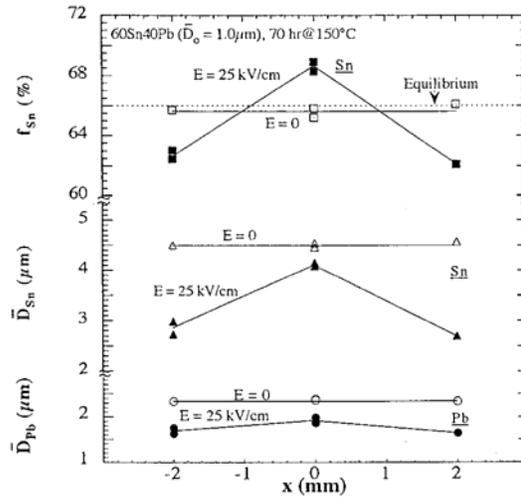
Fig. 9. Gradients in the phase size and volume fraction of the respective phases in 60Sn40Pb solder joints annealed for 70 hr at 150°C without and with an applied electric field E=25 kV/cm.

Fig. 9 shows that besides the variation in phase size from the outer surface to the center of the solder joints there also occurred a difference in their respective volume fractions at these locations. Near the outer surface the volume fraction of the Sn-rich phase

9

was lower than the equilibrium value without a field, while the reverse was true at the center. *These results indicate that the field affected the equilibrium volume fraction of the respective phases in addition to retarding their coarsening rates.* The field also retarded the growth of the intermetallic compounds formed at the solder-Cu substrate.

2.3 Grain Growth: Reducing the grain size of metals generally leads to an increase in strength. As a result there has developed in recent years an increased interest in producing metals with an ultrafine grain size extending down to the nanometer range. However, because of the high energy associated with the grain boundaries, ultrafine-grained metals are usually unstable in that grain growth occurs under otherwise normally stable conditions. Since in prior work by the P.I. and coworkers [7] it was found that the application of an electric field during the annealing of cold-worked Al and Cu wire retarded recovery and recrystallization, the objective of this research activity was to determine whether an electric field might also retard grain growth in ultrafine-grained metals. The material chosen was electrodeposited Cu with an initial as-deposited grain size D=600 nm, which is used in electronic packages.

It was found that the application of an electric fileld during annealing at 150° - 195°C of the electrodeposited Cu retarded grain growth; see Fig 10. An analysis of the kinetics of the grain growth gave

$$dD/dt = A_o \exp(-Q/RT)t^n \qquad (4)$$

with $A_o \approx 10^{-5}$ m/s^n, $Q \approx 11$ kJ/mole and $n \approx 0.06$. It was determined that the retarding effect of the field was through a reduction in A_o and Q, but such that the product $A_o \exp(-Q/RT)$ decreased with field. Further, the results indicated that the driving force for grain growth

10
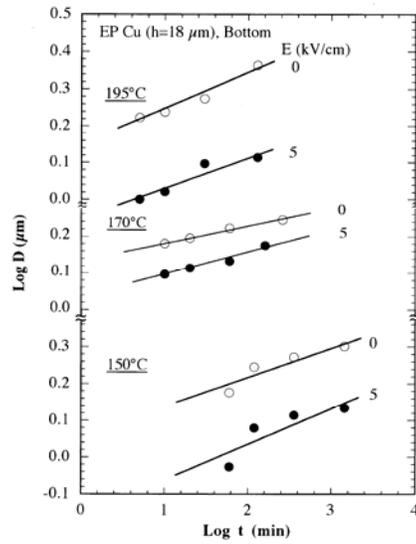
Fig. 10. Log grain size D vs. log annealing time t for 18 μm thick electrodeposited Cu foil annealed at 150°-195°C without and with an electric field E=5 kV/cm. "Bottom" indicates side of the foil adjacent to the sbustrate.

was due to the presence of a high density of dislocations (and other crystal defects),

which decreased with time during the annealing process as a result of their annihilation.

Li's [8] model for this process gives

$$(dD/dt)^{-1}=M^{-1}(P_o^{-1} + k_R t) \qquad (5)$$

where M is the grain growth mobility, P_o the initial driving force and k_R a second order

dislocation annihilation constant. Employing Eqn. 5, the apparent activation energy Q in

Eqn. 4 is the difference between Q_M and Q_R, i.e., $Q=Q_M-Q_R$, where $Q_M≈80$ kJ/mole is the

activation energy for grain boundary mobility (by vacancy migration) and $Q_R≈70$ kJ/mole

that for the annihilation of dislocations. The present data did not provide for an

unequivocal statement regarding the relative effect of the field on Q_M and Q_R, which gave

the reduction in Q.

2.4 Effect of Grain Size on the Flow Stress: Since grain size is important in mechanical

properties, it was deemed desirable as part of our research on the effect of an electric field

11

on grain growth to determine the effect of grain size over the wide range from millimeters to nanometers on the flow stress of metals and metal compounds, and in turn the governing mechanisms. Considered were the FCC metals Cu, Ag and Au, CPH Zn, a BCC Ti-15 at. % Mo alloy and several other metals and compounds including WC and TiN. The metals (Cu and Zn) and the compounds (WC and TiN) were produced with grain size D<10 nm by the Co-PI (J. Narayan) and his colleagues employing a unique pulsed laser vapor deposition technique; see for example Fig. 11.
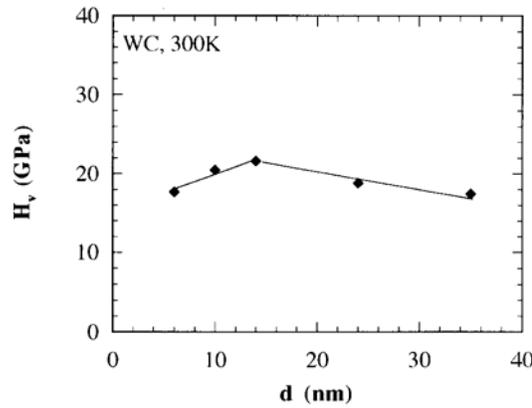

Fig. 11. Hardness H_v vs grain size d showing grain size softening for WC films produced by pulsed laser vapor deposition.

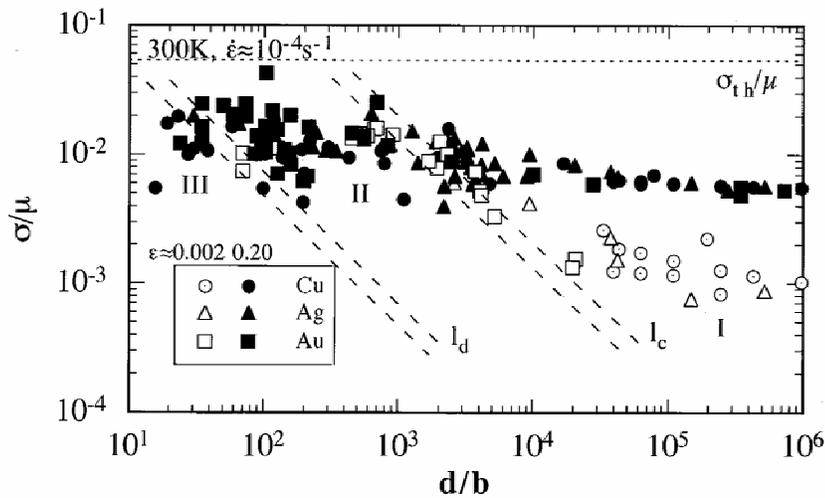

Fig. 12. Log of the modulus-normalized flow stress σ/μ at strains ε=0.002 and 0.20 vs the Burgers vector-normalized grain size d/b for the FCC metals Cu, Ag and Au with grain size in the range from millimeters to nanometers.

As an example, Fig. 12 gives a plot of the modulus-normalized flow stress σ/μ vs. the Burgers vector-normalized grain size d/b for the FCC metals Cu, Ag and Au. Three regimes are identified: (a) Regime I, $d/b \geq \sim 10^4$ m, (b) Regime II, $d/b \approx 10^2$-10^4 m and (c) Regime III, $d/b < \sim 10^2$. Grain size hardening occurred in Regimes I and II, while grain size softening occurred in Regime III. Dislocations were present in Regimes I and II, while they were abscent in Regime III. Seperation between Regimes I and II occurred when the grain size became smaller than the dislocation cell size, separation between Regimes II

Table 2. Proposed physical mechanisms governing the grain size dependence of the flow stress in metals and metal compounds.

Material	Grain Size Regime	Grain Size Hardening or Softening Mechanism	Rate-Controlling Mechanism
Cu, Ag, Au (FCC)	I	Dislocation density hardening	Intersection of dislocations
	II	Disloc. pile-up and grain boundary shear	Grain boundary shear
	III	Grain boundary shear	Grain boundary shear
Zn (CPH)	I	Dislocation density hardening	Intersection of dislocations
	II	Ditto	Ditto
	III	Grain boundary shear	Grain boundary shear
Ti-15at% Mo (BCC)	I	Dislocation density hardening	Overcoming solutes
WC (Hex)	I	Dislocation density hardening or dislocation pile-up	Peierls-Nabarro stress
	II	Ditto	?
	III	Grain boundary shear	Grain boundary shear
TiN (Cubic)	I	?	?
	II	?	?
	III	Texture softening	?
TiAl, ZrTi	III	Grain boundary shear	Grain boundary shear

and III when the grain size became smaller than the elastic interaction spacing between

dislocations. Similar grain size regimes were identified in the other metals and in metal

compounds. A summary of the mechanisms concluded to be governing the grain size

dependence of the flow in each of the three regimes and the corresponding rate-controlling

plastic deformation mechanism are presented in Table 2.

2.5 Consideration of the Physical Basis for the Effect of an Electric Field on Phase

Equilibria and Kinetics in Metals: As pointed out in the Statement of the Problem section,
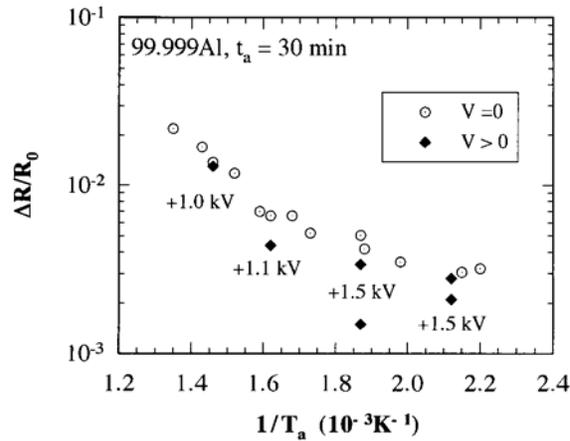
Fig. 13. As-quenched resistivity ratio $\Delta R/Ro$ vs the reciprocal of the annealing temperature
without and with application of an external electric field of ~1 kV/cm.

normally an effect of electric field on solid state phenomena in conductors such as

metals is not expected. An effect could however occur if there exist charged defects (e.g.,

vacancies, dislocations, grain boundaries) within the specimen. The charged crystal defects

could interact directly with the applied electric field or indirectly with the charged exterior

surface produced by the field. The results obtained in the present and previous ARO-

sponsored research suggest that either or both mechanisms could be operative with the

application of an electric field during solid-state phenomena in metals. A speculative

consideration of the interaction between a charged vacancy-solute complex and an

externally applied electric field is given in Appendix III.

Preliminary studies [Fig. 13] indicated that an electric field of the order of a kV/cm had no detectable effect on the concentration of vacancies in high purity Al (99.999) at 200°-500°C. This suggests that the charge on vacancies alone, as contrasted to vacancy-solute complexes, may be insufficient to give a significant change in their concentration with a field of ~1 kV/cm. However, since an electric field produced a significant increase in the solubility of the pertinent alloying constituents in Al-Mg-Si alloys with the presence of excess Si and/or Cu addition, it appears that the charge on vacancy-solute complexes may be of sufficient magnitude for an interaction with the field. *Additional work is needed to determine the effects of an electric field on the concentration and mobility of vacancies in metals and alloys, especially since only very preliminary results (Fig. 13) have been obtained to-date.*

2.6 Novel Microstructures Fabricated by Pulsed Laser Vapor Deposition: Rectifying $La_{0.7}Sr_{0.3}MnO_3$/ZnO (LSMO/ZnO) heterojunctions were grown on a sapphire substrate using a pulsed excimer laser. These junctions provide an effective way to control the electrical and magnetic characteristics of giant magnetoresistive LSMO films by using the built-in electric field at the LSMO/ZnO interface. They also provide an opportunity to investigate various magnetic and magneto-resistive properties of manganites with nonliner optical and optoelectronic applications of ZnO.

Self-assembled, nanocrystalline metal particles (nanodots) were embedded in various ceramic matrices (see for example Fig. 14) employing a novel pulsed laser vapor-deposition technique. Photoluminescence spectra of Au nanodots in ZnO matrix showed
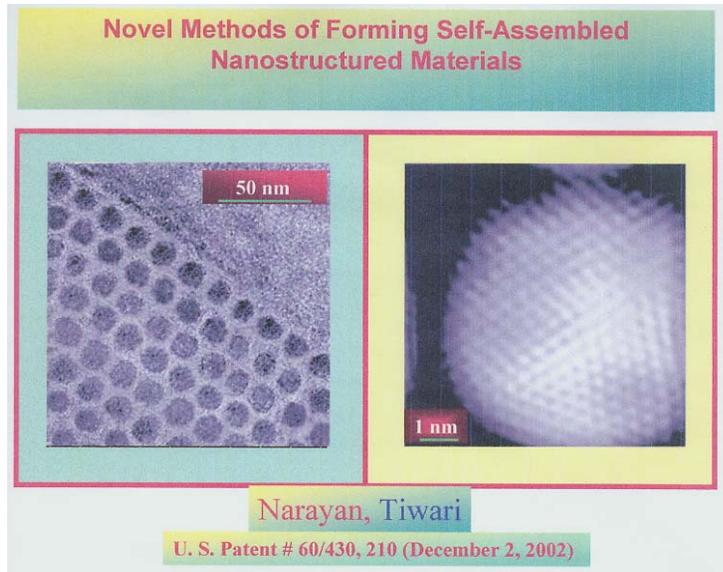
Fig. 12. Nanodot arrays produced by the pulsed laser deposition technique. Left: cross section <110> TEM image of Ni nanodots embedded in alumina matrix on Si (100). Right: high resolution TEM image of one Ni nanodot.

a sharp excitonic peak at 3.22 ± 0.05 eV without any signature of green band emission.

Electrical resistivity measurements showed these films to be highly conducting with a

room temperature resistivity of 3.4 ± 0.2 mΩ-cm.

2.7 Summary of "Firsts": The following are some of the more significant "first time ever results" obtained on the present project.

(1) Determined that an electric field increased the solubility of pertinent alloying

constituents in commercial Al-Mg-Si alloys. The increase in solubility gave an

increase in tensile properties for a given solution heat treatment temperature T_{SHT}, or

allowed for a decrease of 10°-50°C in T_{SHT} and still obtain nominal tensile

properties.

(2) Employing HRTEM and SAED determined for the first time the size distribution and

crystal structure of the precipitates in a naturally-aged Al-Mg-Si alloy.

(3) Determined that an electric field retarded grain growth in ultrafine-grained (D=600

16

nm) electrodeposited Cu. Further, it was shown how the activation energy Q and time exponent n in the grain growth equation were related to: (a) existing crystal defects, (b) their annihilation with time and (c) grain boundary mobility.

(4)   Determined that an electric field influenced phase equlibria and retarded phase coarsening in 60Sn40Pb solder joints.

(5)   Correlated the grain size dependence of the flow stress of a number of metals and compounds over the entire range of the grain size from nanometers to millimeters and proposed the goverening mechanisms.

(6)   Produced "artifact-free" nanocrystalline (including d<10 nm) metals and compounds employing a unique pulsed laser deposition (PLD) technique.

(7)   Fabricated novel materials including metal nanodots in ceramic matrices employing PLD.

2.8 Bibliography

1.   Ø. Gröng, Metallurgical Modeling of Welding, 2nd Ed. The Inst. Of Materials, The Univ. Press, Cambridge (1997) p. 308.

2.   W. A. Johnson and R. F. Mehl, Trans. AIME 135 (1939) 416.

3.   M. V. Avrami, J. Chem. Phys. 7 (1939) 1103.

4.   A. N. Kolmogorov, An. Akad. Nauk, USSR. Ser. Mathemat. 1 (1937) 355.

5.   S. Esmaeili, D. J. Lloyd and W. J. Poole, Acta Mater. 51 (2003) 2243.

6.   Y. Fahmy and H. Conrad, Metal. Mater. Trans. A 32A (2001) 811.

7.   H. Conrad, Z. Guo and A. F. Sprecher, Scripta Metall. 23 (1989) 821.

8.   J. C. M. Li, in Recrystallization, Grain Growth and Textures, ASM, Metals Park, Ohio (1966) pp. 45.

3. List of all publications and technical reports

(a) Papers published in peer-reviewed journals

1. H. Conrad and J. Narayan, "Mechanism for grain size hardening and softening in Zn," Acta Mater. 50 (2002) 5067-5078.

2. H. Conrad and J. Narayan, "Grain size hardening and softening in tungsten carbide at low homologous temperatures," in Electron Microscopy: Its Role in Materials Science, eds. J. K. Weertman, M. Fine, K. Feber, W. King and P. Liaw, TMS, Warrendale, PA (2003) 141-148.

3. K. Jung and H. Conrad, "Effect of an electric field on microstructure coarsening in 60Sn40Pb solder joints," Mater. Sci. Eng. A356 (2003) 8-16.

4. K. Jung and H. Conrad, "Microstructure gradient in 60Sn40Pb solder joints annealed under an electric field," J. Mater. Sci. 39 (2004) 1803-1804.

5. H. Conrad and K. Jung, "Effects of an electric field or current on phase transformations in metals and ceramics," Mater. Mfg. Processes 19 (2004) 573-585.

6. S. D. Antolovich and H. Conrad, "The effects of electric currents and fields on deformation in metals, ceramics and ionic materials," Mater. Mfg. Processes 19 (2004) 587-610.

7. R. W. Armstrong, H. Conrad and F. R. N. Nabarro, "Meso-nanoscopic polycrystal/composite strengthening," in MRS Symp. Q: Mechanical Properties of Nanostructured Materials and Nanocomposites, MRS Symp. Proc. Vol. 791 (2004) Q3.6.1-Q3.6.9.

8. H. Conrad, "Grain size dependence of the flow stress of Cu from millimeters to nanometers," Metal. Mater. Trans. A 35A (2004) 2681-2695.

9. H. Conrad and K. Jung, "Effects of an electric field applied during solution heat treatment of the Al-Mg-Si-Cu alloy AA6111," Zeit für Metallkde. 95 (2004) 352-355.

10. K. Jung and H. Conrad, "External electric field applied during solution heat treatment of the Al-Mg-Si alloy AA6022," J. Mater. Sci. 39 (2004) 6483-6486.

11. H. Conrad and K. Jung, "Influence of an electric field during solution heat treatment of three 6000-series (Al-Mg-Ai) alloys," in Multiphase Phenomena and CDF Modeling in Materials Processes, eds. L. Nastac and B. Q. Li, TMS, Warrendale, PA, (2004) 75-83.

12. H. Conrad and K. Jung, "Effect of grain size from millimeters to nanometers on the flows stress and deformation kinetics of Ag," Mater. Sci. Eng. <u>A391</u> (2005) 272-284.

13. H. Conrad and K. Jung, "On the strain rate sensitivity of the flow stress of ultrafine-grained Cu processed by equal channel angular extrusion (ECAE)," Scripta Mater. <u>53</u> (2005) 581-584.

14. H. Conrad, J. Narayan and K. Jung, "Grain size softening in nanocrystalline TiN," Int. J. Refract. Met. Hard Mater. <u>23</u> (2005) 301-305.

15. H. Conrad, "Enhanced phenomena in metals with electric and magnetic fields: I Electric Fields," Mater. Trans. Japan Inst. Met. <u>46</u> (2005) 1-5.

16. H. Conrad and K. Jung, "Effect of grain size from mm to nm on the flows stress and plastic deformation kinetics of Au at low homologous temperatures," Mater Sci. Eng. <u>A406</u> (2005) 78-85.

17. K.-H. Chia, K. Jung and H. Conrad, "Dislocation density model for the effect of grain size on the flow stress of Ti-15.2 at. % Mo β-alloy at 4.2-650K," Mater. Sci. Eng. A, in print.

18. K. Jung and H. Conrad, "Effect of electric field strength applied during the solution heat treatment of the Al-Mg-Si-Cu alloy AA6111," Zeit für Metallkde, in print.

19. H. Conrad and K. Jung, "Effects of grain size from millimeters to nanometers on the flow stress of metals and compounds," J. Electronic Mater., in print.

20. A. Tiwari, C. Jin, D. Kumar and J. Narayan, "Rectifying electrical characteristics of $La_{0.7}Sr_{0.3}MnO_3$/ZnO heterostructure," Appl. Phys. Lett. <u>83</u> (2003) 1773-1775.

21. A. Tiwari, A. Chugh, C. Jin and J. Narayan, "Role of self-assembled Au nanodots in improving the electrical and optical characteristics of ZnO films," J. Nanosci. Nanotech. <u>3</u> (2003) 368-371.

22. J. Narayan and A. Tiwari, "Novel methods of forming self-assembled nanostructured materials," J. Nanosci. Nanotech. <u>4</u> (2004) 726-732.

23. J. Narayan, "New frontiers in thin film growth and nanomaterials," 2004 Edward De Mille Campbell Memorial Lecture, ASM, Metall. Mater. Trans A <u>36A</u> (2005) 277-294.

<u>(b) Papers published in non-peer reviewed journals or in conference proceedings</u>

1. H. Conrad and K. Jung, "On the so-called inverse Hall-Petch effect in nanocrystalline

metals and metal compounds," In <u>11th Int. Conf. Composites/Nano Engineering, (ICEE -11)</u>, D. Hui, ed., College Engr., New Orleans (2004) 113-114.

2. R. W. Armstrong and H. Conrad, "Micro-to-nanostructure modeling of composite material deformation and fracturing properties II," In <u>11th Int. Conf. Composites/Nano Engineering, (ICEE -11)</u>, D. Hui, ed., College Engr., New Orleans (2004) 23-24.

<u>(c) Papers submitted at meetings, but not yet published in conference proceedings</u>

None.

<u>(d) Manuscripts submitted but not yet published</u>

1. H. Conrad and K. Jung, "On the anomalous stress-dependence of the activation volume in Cu with a submicron grain size," submitted to Scripta Met.

2. H. Conrad and K. Jung, "Effect of an electric field applied during the solution heat treatment of the Al-Mg-Si alloy AA6022 on the subsequent natural aging kinetics," submitted to J. Mater. Sci.

3. K. Jung and H. Conrad, "Effects of an electric field applied during the solution heat treatment of the Al-Mg-Si-Cu alloy AA6111 on the subsequent natural aging kinetics and tensile properties," submitted to Zeit. Für Metallkde.

4. K. Jung and H. Conrad, "Retardation of grain growth in electrodeposited Cu by an electric field," submitted to Scripta Mater.

5. S. Ramachandran, K. Jung, J. Narayan and H. Conrad, "HRTEM observations on the precipitates in naturally-aged Al-Mg-Si alloy AA6022," submitted to Scripta Mater.

6. H. Conrad, S. Ramachandran, K. Jung and J. Narayan, "HRTEM observations on the microstructure of naturally-aged Al-Mg-Si alloy AA6022 processed with an electric field," submitted to J. Mater. Sci.

7. H. Conrad and K. Jung, "Application of an Electric Field during Processing of Automotive Al Sheet Alloys" (Invited), to be submitted to Thermac' 2006 to be held in Vancouver July 4-8, 2006.

<u>(e) Technical reports submitted to ARO</u>

1. H. Conrad, J. Narayan and K. Jung, Annual report for the period 7/22/02-12/31/02 on DAA19-02-1-0315, 41893-MS. Report Date: 12/31/02.

2. H. Conrad, J. Narayan and K. Jung, Annual report for the period 1/01/03-12/31/03 on

DAA19-02-1-0315, 41893-MS. Report Date: 12/31/03.

3.   H. Conrad, J. Narayan and K. Jung, Interim progress report for the period 1/01/04-07/31/04 on DAA19-02-1-0315, 4183-MS. Rept. Date 09/20/2004.

4.   H. Conrad, J. Narayan and K. Jung, Interim progress report for the period 07/22/02-07/31/04 on DAA19-02-1-0315, 4183-MS. Rept. Date 10/06/2004.

4. Participating Scientific Personnel

1.   Prof. H. Conrad, P.I.

2.   Prof. J. Narayan, Co-P.I.

3.   Dr. K Jung, post-doctoral fellow

4.   S. Ramachandren, graduate student, passed PhD qualifying exam

5.   Wes Crill, undergraduate student, received B.S. degree; enrolled in graduate school.

5. Report of Inventions

a.   J. Narayan and A. Tiwari, "Method for forming three-dimensional nanodot arrays in a matrix," US Patent Pending (2004).

6. Technology Transfer

(a) H. Conrad

(1)   Through visits, seminar presentations and communications have maintained cntinued interactions with the Al industry (Dr. D. Lloyd, Alcan, Dr. R. Ramage, Alcoa, and Dr. B. Das, Secat) and the automotive industry (Drs. M. Demeri and A. Sherman, Ford Scientic Laboratory) regarding results and potential benefits of applying an electric field in the processing of Al alloys.

(2)   Initiated with Dr. R. Becher, ORNL, a research project on the effect of an electric field on the plastic deformation of oxide ceramics.

(3) Upon invitation gave a seminar on our work and spent several days with Drs. R.
Armstrong, J. House and R. DeAngelis, Materials Laboratory, Eglin Air Force
Base, FL. discussing mutual research activities including the effects of electric
fields on metals and ceramics.

(4) Developed interactions with Dr. H. Merchant, Gould Electronics, regarding the
influence of an electric field on the properties of electrodeposited Cu used in
electronic packages.

Appendix I: Calculation of the effect of electric field on the thermodynamic solubility parameters determined from resistivity ρ measurements

$$\rho_s = \rho_w - \rho_o = \alpha c^n = \alpha \exp\text{-}(\Delta G_s/RT)^n \qquad (\text{I-1})$$

$$= \alpha \exp(n\Delta S_s/R)\exp\text{-}(n\Delta H_s/RT) \qquad (\text{I-1a})$$

$$= \beta \exp\text{-}(Q/RT) \qquad (\text{I-2})$$

ρ_o = resistivity due to insoluble constituents; c is the concentration of the soluble constituents, ρ_s the resistivity due to the soluble constituents, ρ_w that of the as-quenched state and ΔH_s, ΔS_s and ΔG_s are the enthalpy, entropy and Gibbs free energy of solution. α and n are constants.

- Knowing ΔH_s and ΔS_s for E=0 (from Gröng [1]) we can obtain the effect of E_{SHT} on c from a plot of ρ_s vs. $1/T_{SHT}$.

Appendix II: Analysis of natural aging kinetics of the Al-Mg-Si alloys in terms of the Johnson- Mehl, Avrami, Kolmogorov (JMAK) model

- The JMAK model gives

$$f_r = 1 - \exp(-k t_{NA}^n) \tag{II-1}$$

   f_r=relative volume fraction of precipitate, t_{NA}=natural aging time, k and n are

   constants.

- f_r is given by

$$f_r = f_c / f_c^* = \rho_c / \rho_c^* \tag{II-2}$$

   f_c=actual volume traction of precipitate at t_{NA}, and f_c^* that at the peek-aged state.

   ρ_c=resistivity due to the precipitate at t_{NA} and ρ_c^* that at the peak-aged state.

- Assume $\qquad\qquad\qquad\quad \rho = \rho_o + \rho_c + \rho_s \tag{II-3}$

   ρ_o=resistivity of Al matrix, ρ_c that due to precipitate and ρ_s that due to solutes

   remaining in solution.

- One then obtains $\rho_c = (\rho - \rho_w)/(1-\alpha)$ and $\rho_s = (\rho_w - \rho_o) - \alpha\rho_c$, so that

$$f_r = [(\rho - \rho_w)/ (1-\alpha)(\rho^* - \rho_o)] \tag{II-4}$$

   $\alpha = \rho_s/\rho_c$ and ρ^* is the resistivity of the peak-aged state.

- Rearranging Eqn. 1 and taking double logarithms gives

$$\ln \ln [1/(1 - f_r)] = \ln k + n \ln t_{NA} \tag{II-5}$$

   or $\qquad\qquad \log \log[1/(1 - f_r)] = \log(k/2.3) + n \log t_{NA} \tag{II-5a}$

- Insert Eqn. II-4 for f_r into Eqn. II-5a and plot left hand side of Eqn. II-5a vs log t_{NA}

   to obtain n from the slope and k from the intercept of the line.

Appendix III: Simplified and Speculative Model for the Effect of an Electric Field on Solubility of Si in Al

Based on: A.D. LeClaire (1978) and Shewmon (1989)

- Vacancy with electron cloud results in negative charge on the vacancy.
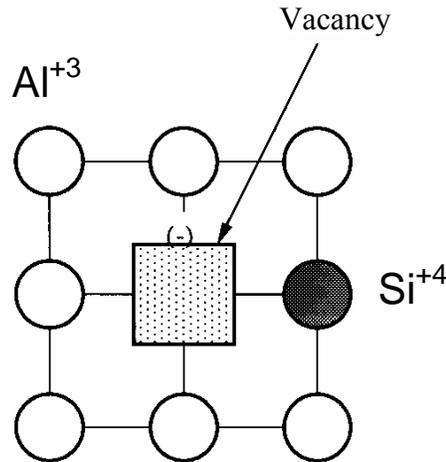
- Attractive force between negatively-charged vacancy and positively-charged Si ion gives binding energy E_b.

- Energy of vacancy thus decreases and their concentration increases.

$$C_v = A\exp\text{-}[(E_v^f\text{-}E_b)/kT] \tag{III-1}$$

- Electrostatic potential V(r) around the solute ion is

$$V(r) = (Ze/r)\exp\text{-}q(r) \tag{III-2}$$

  Z=No. of excess electrons per ion
  e=Charge on an electron
  q=Screening parameter
  r=Radial distance from ion

- Effect of electric field E

$$V_E(r) = [(Ze/r)\exp\text{-}q(r)]\text{-}Ex \tag{III-3}$$

  x=distance over which the electric field acts

Refs.
A. D. LeClaire, J. Nucl. Mater. <u>69&70</u> (1978) 82.

P. Shewmon, <u>Diffusion in Solids</u>, 2nd. Ed. TMS, Warrendale, PA (1989) p. 104-107.